Interactions between the Cytochrome *b*, Cytochrome c_1, and Fe−S Protein Subunits at the Ubihydroquinone Oxidation Site of the bc_1 Complex of *Rhodobacter capsulatus*†

A. Sami Sarıbaş,‡ Maria Valkova-Valchanova,‡ Mariko K. Tokito,‡,§ Zhaolei Zhang,|| Edward A. Berry,|| and Fevzi Daldal*,‡

Department of Biology, Plant Science Institute, University of Pennsylvania, Philadelphia, Pennsylvania 19104, and Lawrence Berkeley National Laboratory, 1 Cyclotron Road, Berkeley, California 94720

Received December 23, 1997; Revised Manuscript Received April 6, 1998

ABSTRACT: Ubihydroquinone:cytochrome (cyt) *c* oxidoreductase (bc_1 complex and its plant counterpart b_6f complex) is a vital component of energy-transducing systems in most organisms from bacteria to eukaryotes. In the facultative phototrophic (Ps) bacterium *Rhodobacter capsulatus*, it is constituted by the cyt *b*, cyt c_1, and Rieske Fe−S protein subunits and is essential for Ps growth. Of these subunits, cyt *b* has two nontransmembrane helices, *cd*1 and *cd*2, which are critical for its structure and function. In particular, substitution of threonine (T) at position 163 on *cd*1 with phenylalanine (F) or proline (P) leads to the absence of the bc_1 complex. Here, Ps^+ revertants of B:T163F were obtained, and their detailed characterizations indicated that position 163 is important for the assembly of the bc_1 complex by mediating subunit interactions at the Q_o site. The loss of the hydroxyl group at position 163 of cyt *b* was compensated for by the gain of either a hydroxyl group at position 182 of cyt *b* or 46 of the Fe−S protein or a sulfhydryl group at position 46 of cyt c_1. Examination of the mitochondrial bc_1 complex crystal structure [Zhang, Z., Huang, L., Shulmeister, V. M., Chi, Y.-I., Kim, K. K., Hung, L.-W., Crofts, A. R., Berry, E. A., and Kim, S.-H. (1998) *Nature 392*, 677−684] revealed that the counterparts of B:G182 (i.e., G167) and F:A46 (i.e., A70) are located close to B:T163 (i.e., T148), whereas the C:R46 (i.e., R28) is remarkably far from it. The revertants contained substoichiometric amounts of the Fe−S protein subunit and exhibited steady-state and single-turnover, electron transfer activities lower than that of a wild-type bc_1 complex. Interestingly, their membrane supernatants contained a smaller form of this subunit with physicochemical properties identical to those of its membrane-bound form. Determination of the amino-terminal amino acid sequence of this soluble Fe−S protein revealed that it was derived from the wild-type protein by proteolytic cleavage at V44. This work revealed for the first time that position 163 of cyt *b* is important both for proper subunit interactions at the Q_o site and for inactivation of the bc_1 complex by proteolytic cleavage of its Fe−S protein subunit at a region apparently responsible for its mobility during Q_o site catalysis.

Ubihydroquinone:cytochrome (cyt)[1] *c* oxidoreductase (bc_1 complex and its plant counterpart b_6f complex) is an important energy transduction complex in most organisms from bacteria to eukaryotes. In purple non-sulfur photosynthetic bacteria like *Rhodobacter capsulatus*, it conveys electrons from ubihydroquinone to both cyt c_2 and c_y and contributes to the formation of a proton gradient subsequently used for ATP production (for recent reviews, see refs *1*−*3*).

In most bacteria, the bc_1 complex is composed of the Rieske Fe−S protein, cyt *b*, and cyt c_1 subunits encoded by *fbcF*/*petA*, *fbcB*/*petB*, and *fbcC*/*petC* genes organized as an operon (see for a review ref *3*). Cyt *b* is a highly conserved integral membrane protein (*4*) which bears two heme groups, b_L and b_H with low and high redox midpoint potential (E_{m7}) values, respectively. Both the Fe−S protein which contains a [2Fe-2S] cluster which can be detected by EPR spectroscopy in its reduced form and cyt c_1 which has a covalently attached heme group are membrane-anchored and face the periplasm. Oxidation of ubihydroquinone and reduction of ubiquinone take place in two distinct domains of the bc_1

† This work was supported by NIH Grants GM 38237 to F.D. and DK44842 to E.A.B.

* To whom correspondence should be addressed. Phone: (215) 898-4394. Fax: (215) 898-8780. E-mail: fdaldal@.sas.upenn.edu.

‡ University of Pennsylvania.

§ Present address: Department of Animal Biology, Veterinary School of the University of Pennsylvania, Philadelphia, Pennsylvania 19104.

|| Lawrence Berkeley National Laboratory.

[1] Abbreviations: cyt, cytochrome; bc_1 complex, ubihydroquinone cytochrome *c* oxidoreductase; QH_2, ubihydroquinone; Q, ubiquinone; Q_o, ubihydroquinone oxidation site; Q_i, ubiquinone reduction site; [2Fe-2S], two iron−two sulfur cluster of the Rieske Fe−S protein; EPR, electron paramagnetic resonance; b_L, low-potential *b*-type heme; b_H, high-potential *b*-type heme; E_h, ambient potential; E_{m7}, redox midpoint potential at pH 7.0; Ps, photosynthesis; Res, respiration; SDS−PAGE, sodium dodecyl sulfate−polyacrylamide gel electrophoresis; ONPG, *o*-nitrophenyl β-galactoside; X-gal, bromo-4-chloro-3-indolyl β-D-galactoside; DAD, 2,3,5,6-tetramethyl-*p*-phenylenediamine; PMS, *N*-methyldibenzopyrazine methosulfate; PES, *N*-ethyldibenzopyrazine ethosulfate; MOPS, (*N*-morpholino)propanesulfonic acid; TMPD, *N*,*N*,*N*′,*N*′-tetramethyl-*p*-phenylenediamine; 1,2-NQ-4S, 1,2-naphthoquinone-4-sulfonic acid; EDTA, ethylenediaminetetraacetic acid; PMSF, phenylmethanesulfonyl fluoride; DBH, 2,3-dimethoxy-5-decyl-6-methyl-1,4-benzohydroquinone; SHE, standard hydrogen electrode.

S0006-2960(97)03146-2 CCC: $15.00
Published on Web 05/12/1998

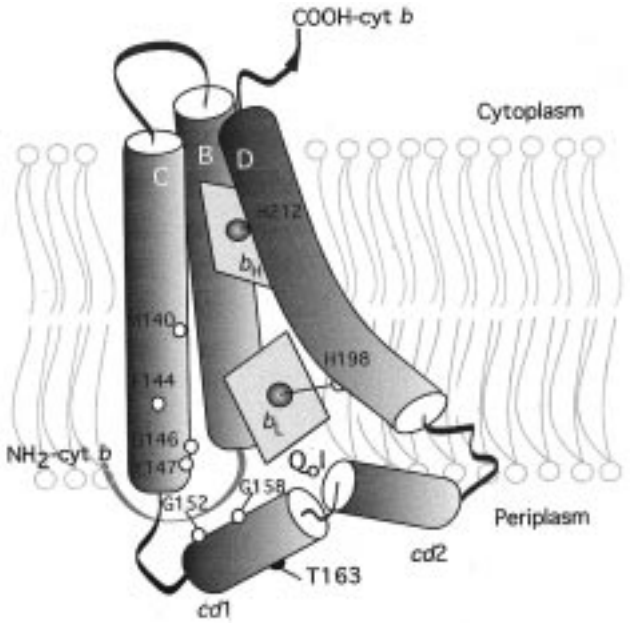

FIGURE 1: Cartoon model of the Q_oI region of cyt *b* and location of the T163 residue. Only the B−D transmembrane and the *cd*1 and *cd*2 non-transmembrane helices of cyt *b* are shown as gray cylinders. The functionally important residues M140, F144, G146, Y147, G152, and G158 and the heme b_H and b_L ligands H198 and H212 are indicated. Heme porphyrins and Fe atoms are depicted as diamonds and spheres, respectively. NH_2 and COOH indicate the amino and carboxyl ends of cyt *b*.

complex, called Q_o and Q_i sites. These sites are located near the hemes b_L and b_H on the outer and inner sides of the cytoplasmic membrane, respectively. Earlier indications about the location of these sites within the bc_1 complex came from genetic analysis of spontaneous inhibitor resistance mutations in several species, mainly in yeast and bacteria (for a review, see ref *5*). In the case of the Q_o site, most of these mutations were confined to a highly conserved portion of cyt *b* called the Q_oI domain encompassing residues M140−T163 (*6*) (Figure 1). The Q_oI domain is located between helices C and D of cyt *b* and bears a structural resemblance to the quinone binding (Q_A and Q_B) domains of the bacterial photosynthetic reaction center (RC) (*7*). Biochemical, biophysical, and genetic studies have revealed that residues F144, G152, and G158 affect the Q/QH_2 occupancy of the Q_o site (*7*−*11*), that M140 and Y147 are essential for electron transfer from the Q_o site to the [2Fe-2S] cluster and to cyt b_L (*12*), and that G146 is critical for proper packing of heme b_L (*13*) (Figure 1).

The mitochondrial bc_1 complexes from both chicken heart and bovine heart have been crystallized (*14*−*16*), and their complete structures are now solved (*17*, *45*). With respect to cyt *b*, the structure has confirmed the previously predicted eight transmembrane helices structure (for a review, see ref *1*) and further revealed the presence of two non-transmembrane helices (*cd*1 and *cd*2) around the Q_o site (*17*, *45*). A great deal of structural information, such as the distances between the redox centers in the bc_1 complex, is now available. Unexpectedly, it was found that the Fe−S protein can occupy distinct positions in different crystals of the bc_1 complex, hinting at its mobility (*17*−*19*, *45*).

Currently, there is a fair amount of data about the role of several residues affecting Q/QH_2 binding or electron transfer reactions at the Q_o site (reviewed in ref *5*). However, little is known about the residues coordinating the protein interactions between the subunits and their postulated movement during catalysis. The nature of the electronic events within the bc_1 complex and the available data clearly suggest that the Q_oI region of cyt *b* interacts with the [2Fe-2S] cluster region of the Fe−S protein around non-transmembrane helices *cd*1 and *cd*2 (Figure 1). Indeed, a few mutations located in the Q_oI domain have been found to affect binding of the Fe−S protein to the cyt *b* subunit in yeast (*20*), or of the accessory fourth subunit in *Rhodobacter sphaeroides* (*21*). Furthermore, it has been shown that mutants lacking the Fe−S protein subunit still form a cyt *b*−cyt c_1 subcomplex (*22*), which can be purified as a reconstitutively active entity (M. Valkova-Valchanova et al., in preparation). On the other hand, mutants lacking cyt *b* yield only low amounts of cyt c_1, and those without cyt c_1 contain no bc_1 complex in their cytoplasmic membranes (*23*).

An important insight into the formation of the Q_o site became available by the observation that among the many Q_oI region mutants only the B:T163F and -P substitutions abolished the assembly of the bc_1 complex (*9*). This finding, in light of the work of Davidson et al. (*23*), strongly suggested that these mutations must also perturb the interactions between cyt *b* and cyt c_1 subunits, since otherwise they would have contained a cyt *b*−cyt c_1 subcomplex. Revertants of the B:T163F mutation were therefore selected, and the intragenic and intergenic second-site suppressors located in cyt *b*, cyt c_1, and the Fe−S protein were characterized in detail. The double mutants contained considerable amounts of a soluble, truncated form of the Rieske Fe−S protein with wild-type physicochemical properties. These findings indicated for the first time that non-transmembrane helix *cd*1 of cyt *b* is critical not only for the assembly of the bc_1 complex but also for its proteolytic inactivation via cleavage of the Fe−S protein subunit at a region thought to be important for its mobility during Q_o site catalysis.

MATERIALS AND METHODS

Growth Conditions and Strains. *R. capsulatus* and *Escherichia coli* strains were grown in MPYE and LB media, respectively, supplemented with appropriate antibiotics as needed (*24*). The strains that were used are listed in Table 1.

Preparation of R. capsulatus Electrocompetent Cells and Electroporation. *R. capsulatus* strains (MT1131 and its derivatives) were grown in MPYE medium until an OD_{630} of 0.4−0.5 was reached for the preparation of electrocompetent cells and harvested by centrifugation at room temperature for 10 min at 5 K. They were washed twice with sterile double-distilled water and once with 10% glycerol. The final pellet was resuspended in 10% glycerol, distributed into 200 μL aliquots, rapidly frozen in a dry ice−ethanol bath, and stored at −80 °C. For electroporation, 40 μL of competent cells (in a 0.2 cm gap cuvette) and 10−100 ng of plasmid DNA isolated from *R. capsulatus* were incubated for 10 min at 4 °C. After electroporation with a Bio-Rad Gene Pulser set at 25 mF, 2.5 kV, and 400 W with a time constant of >8, cells were incubated in MPYE medium supplemented with 10 mM $MgCl_2$ and 10 mM $MgSO_4$ for 4 h at 35 °C, centrifuged at 4 K for 5 min,

Table 1: Properties of the Ps^+ Revertants of the B:T163F Mutant of *R. capsulatus* and Its Derivatives

				$Q_o \rightarrow$ cyt b_H[d]		$Q_o \rightarrow$ cyt c[d]	
strain	phenotype (dt in min)[c]	DBH2 (%)	assembly	rate (s^{-1})	E_h (mV)	rate (s^{-1})	E_h (mV)
pMT0-404/MT-RBC1[a]	Ps^+ (120)	100[b]	As^+	500/118	116/208	240	106
MT-RBC1[a]	Ps^- (na)	−	na[c]	na		na	
pB:T163F/MT-RBC1[c]	Ps^- (na)	0	As^-	na		na	
p(B:T163F+B:G182S)/MT-RBC1	Ps^+ (170)	3	As^+	108/38	100/180	55	100
p(B:T163F+C:R46C)/MT-RBC1	Ps^+ (210)	3	As^+	98/35	106/200	45	106
p(B:T163F+F:A46T)/MT-RBC1	Ps^+ (150)	21	As^+	320/64	100/200	185	103
pB:G182S/MT-RBC1	Ps^+ (140)	20	As^+	203/87	100/190	108	100
pC:R46C/MT-RBC1	Ps^+ (190)	32	As^+	390/132	100/200	212	100
pF:A46T/MT-RBC1	Ps^+ (140)	92	As^+	247/52	100/220	155	100

[a] The plasmid pMT0-404 contains the wild-type *fbcFBC* operon, and MT-RBC1 carries a chromosomal deletion of it (*8*). As^+ and As^- indicate the presence and absence of the bc_1 complex in chromatophore membranes, respectively. [b] DBH2 indicates the cyt *c* reductase activity measured using chromatophore membranes, and 100% corresponds to 6272 nmol of horse heart cyt *c* reduced per minute per milligram of total proteins (average of three measurements). [c] This strain was described in ref *9*. dt is the doubling time. na, not applicable. [d] The electron transfer rates were obtained by fitting the flash-induced traces at ΔA (560 − 570 nm) for cyt b_H and at ΔA (550 − 540 nm) for cyt *c* to a single-exponential equation, and the corresponding ambient redox potentials are also indicated.

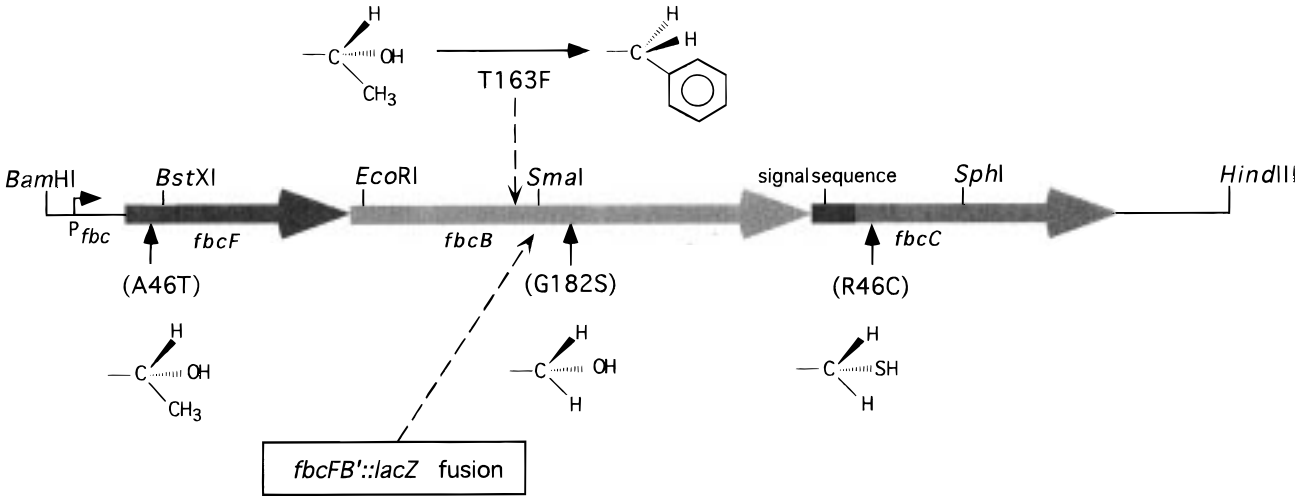

FIGURE 2: Locations of the second-site revertants of the B:T163F mutant in *fbcFBC*. *fbcF*, *fbcB*, and *fbcC* correspond to the structural genes for the Fe−S protein, cyt *b*, and cyt c_1 subunits of the bc_1 complex, respectively. The B:G182S, F:A46T, and C:R46C mutations are the intragenic and extragenic suppressors of B:T163F, determined as described in Materials and Methods. The chemical structures of the amino acid side chains substituting at these positions are also shown. The *Bam*HI−*Sma*I fragments carrying the expression region of *fbcFBC* (P_{fbc}) and the wild-type (B:T163) or the B:T163F mutation were cloned upstream of the promoterless *lacZ* in pGD499 to produce the *fbc*FB′::*lacZ* and *fbc*FB(T163F)′::*lacZ* transcriptional fusions (shown by an arrow) as described in Materials and Methods.

resuspended in 100 μL of MPYE medium, spread on MPYE plates, and incubated under selective growth conditions.

Isolation and Analysis of Ps^+ Revertants of the B:T163F Mutant of R. capsulatus. A total of 1790 spontaneous Ps^+ revertants of the B:T163F mutant (*9*) were isolated from six independent cultures on MPYE plates supplemented with tetracycline and pooled together. Their plasmid DNA was extracted and electroporated into the *R. capsulatus* strain MT-RBC1, and the Ps^+ colonies thus obtained were repooled for plasmid DNA preparation. The *Bst*XI−*Eco*RI, *Eco*RI−*Sty*I, and *Sty*I−*Stu*I fragments containing almost the entire *fbcF*, *fbcB*, and *fbcC* genes were purified by gel electrophoresis from this pooled DNA and exchanged with their appropriate counterparts on pPET-B:T163F containing the B:T163F mutation (*9*). After subsequent ligation to pRK404 and conjugation into MT-RBC1, five independent Ps^+ colonies were retained in each case, and the fragments thus exchanged were resequenced to confirm the presence of the B:T163F mutation and to identify the nature of the additional mutation conferring the Ps^+ phenotype. These analyses revealed that the clones obtained using the *Bst*XI−*Eco*RI, *Eco*RI−*Sty*I, and *Sty*I−*Stu*I DNA fragments contained a single mutation at position 46 [Ala(GCC) to Thr(**A**CC)] of the Fe−S protein (*fbcF*), 182 [Gly(GGC) to Ser(**A**GC)] of cyt *b* (*fbcB*), and 46 [Arg(CGC) to Cys (**T**GC)] of cyt c_1 (*fbcC*), respectively (Figure 2). These plasmids were designated p(B:T163F+B:G182S), p(B:T163F+C:R46C), and p(B:T163F+F:A46T); their *fbcFBC* operons were resequenced to ensure that the second-site revertants (B:T163F+B:G182S, B:T163F+C:R46C, and B:T163F+F:A46T) contained only these mutations.

Construction of the Single Mutants Carrying Only the Second-Site Suppressor Mutations. For the *fbcF*:A46T mutation, the 530 bp *Bst*XI−*Eco*RI fragment and, for the *fbcB*:G182S and *fbcC*:R46C mutations, the 1430 bp *Sma*I−*Sph*I fragment were excised from appropriate plasmids and exchanged with their counterparts on pPET1 bearing a wild-type copy of *fbcFBC* (*8*). The plasmids thus obtained were designated pPET-F:A46T, pPET-B:G182S, and pPET-C:R46C, respectively, ligated into pRK404 using their unique *Hin*dIII restriction site, and introduced into *R. capsulatus* strain MT-RBC1 via triparental crosses selecting for Tet^R.

Construction of the fbcFB′::lac Z Fusions and β-Galactosidase Assays. For the *fbcFB′*::*lacZ* operon fusions, the

promoter-cloning vector pGD499 (*25*) was digested with *Hin*dIII and treated with mung bean nuclease. The blunt-ended vector DNA was then digested with *Bam*HI, and the 29.1 kb DNA fragment containing a promoterless *lac*Z gene was isolated by using "elutips" according to the manufacturer's instructions (Schleicher and Schuell, Keen, NH). It was then ligated to the purified 1.7 kb *Bam*HI−*Sma*I fragments isolated from the appropriate plasmids, pMTS1 (wild-type) (*12*) and its derivative carrying B:T163 which contained the promoter of *fbcFBC*, the entire *fbcF*, and part of *fbcB* (Figure 2). The plasmids thus obtained, p*SmaFB′-Z* and p*SmaFB*(T163F)*′-Z*, were introduced into *E. coli* HB101 cells using $CaCl_2$ transformation and conjugated into MT-RBC1 selecting for Tet^R. The β-galactosidase activity of these transconjugants was monitored by the appearance of a blue color on MPYE plates containing X-Gal. Appropriate isolates were grown in MPYE liquid medium supplemented with tetracycline. Cells were then harvested at an OD_{630} of 0.45−0.48, resuspended in a phosphate buffer (60 mM Na_2HPO_4, 40 mM $NaH_2PO_4{\cdot}H_2O$, 10 mM KCl, 2 mM $MgSO_4$, and 0.25% β-mercaptoethanol), and sonicated briefly. Cell debris was eliminated by centrifugation at 14000*g* using a microfuge, and 100 μL aliquots of the supernatants were assayed using ONPG (4 mg/mL). Development of the yellow color was monitored at 420 nm, and the reaction was stopped after incubation for 2−4 min (vs 20−25 min for the background) at 35 °C by addition of 1 mL of 1 M sodium carbonate. The β-galactosidase specific activity was calculated as millimoles of ONPG hydrolyzed per minute per milligram of total proteins.

Preparation of Chromatophore Membranes and Supernatants. Chromatophore membranes were prepared in 50 mM MOPS (pH 7.0) buffer containing 100 mM KCl, 1 mM PMSF, and 1 mM EDTA using a French pressure cell as described earlier (*8*), except that for spectroscopic analyses they were washed three times with the same buffer. Bacteriochlorophyll and protein concentrations were determined spectrophotometrically using an ϵ_{775} of 75 mM^{-1} cm^{-1} and according to Lowry et al. (*26*), respectively. Membrane-free supernatants were prepared by extensive ultracentrifugation of chromatophore membrane supernatants (spun twice for 16 and 5 h, respectively, at 4 °C and 258000*g*) to ensure that all membrane debris was eliminated. They were then concentrated about 15-fold by using Amicon Centriprep 3 concentrators with a molecular mass cutoff of 3000 Da.

SDS−PAGE and Western Blot Analysis. Laemmli-type SDS−PAGE (with a 15 or 17% acrylamide concentration) was used to analyze the presence of the bc_1 complex subunits in chromatophore membranes and their supernatants. After being stained with Coomassie blue, gels were scanned with a Molecular Dynamics Personal Scanner and analyzed using the IP-GEL documentation software (Molecular Dynamics). Western blot analyses were performed as described in Atta-Asafo-Adjei and Daldal (*8*) using antibodies raised against the Fe−S protein cyt *b* and cyt c_1 subunits of the *R. capsulatus* bc_1 complex.

Flash-Activated Single-Turnover Kinetics. Q_o site catalysis was monitored by flash-activated, time-resolved single-turnover kinetics essentially as described earlier (*27*), except that a single wavelength spectrophotometer was used (Biomedical Instrumentation Group, University of Pennsylvania, Philadelphia, PA). Flash-induced (8 μs actinic light pulse) cyt b_H and cyt *c* re-reduction kinetics were measured using chromatophore membranes which contained approximately 0.20 μM bacterial RC, in the presence of 3 μM valinomycin, 2.5 μM PMS, 2.5 μM PES, 6 μM DAD, 10 μM 2-hydroxy-1,4-naphthoquinone, and 10 μM $FeCl_3$−EDTA. The RC concentration was determined by measuring the optical absorption difference between 605 and 540 nm after four flashes at an E_h of 370 mV and using an extinction coefficient ϵ_{605} of 29.8 mM^{-1} cm^{-1}. Samples were poised at desired E_h values using sodium dithionite or potassium ferricyanide, and the bc_1 complex inhibitors antimycin A (10 μM) and myxothiazol (5 μM) were added as needed. Cyt *b* reduction and cyt *c* re-reduction were monitored at 560 *minus* 570 nm and 550 *minus* 540 nm, respectively, and the single-turnover electron transfer rates were calculated as in Gray et al. (*27*).

EPR Spectroscopy. The soluble and membrane-bound forms of the Fe−S protein in chromatophore membranes and their supernatants of the B:T163F+B:G182S mutant were titrated in the presence of 10 μM TMPD and 50 μM 1,2-NQ-4S between the E_h values of 200 and 400 mV, and the amplitudes of the g_y signals were normalized and used to calculate the E_{m7} values of their [2Fe-2S] clusters. In general, chromatophore membranes of the revertants and single mutants were prepared for EPR spectroscopy with the addition of 20 mM sodium ascorbate. The measurements were carried out using a Bruker spectrometer model ESP-300E, equipped with a helium cryostat under the following conditions: temperature, 20 K; microwave power, 2−5 mW; modulation amplitude, 12.5−20 G; modulation frequency, 100 kHz; and microwave frequency, 9.4 GHz.

Chemicals. PMS, PES, 3,5,6-trimethyl-*p*-phenylenediamine (diaminodurene), antimycin A, myxothiazol, stigmatellin, 2-hydroxy-1,4-naphthoquinone, and pyocyanine were obtained as described earlier (*27*), and oligonucleotides were synthesized by the Nucleic Acid Synthesis Facility of the University of Pennsylvania (Philadelphia, PA). All other chemicals were reagent grade and were purchased from commercial sources.

RESULTS

The Absence of the bc_1 Complex in the B:T163F Mutant Is Not a Consequence of the Transcriptional Polarity of This Mutation. First, the transcriptional fusions p*SmaFB′-Z* and p*SmaFB*(T163F)*′-Z* described in Materials and Methods were used to probe for any transcriptional effect of the B:T163F mutation (Figure 2). These constructs were introduced into the *R. capsulatus* strain MT-RBC1 [Δ(*fbcFBC*)] (Table 1), and the transconjugants obtained were assayed for their β-galactosidase activities. Both of the strains produced similar amounts of such activity (data not shown), indicating that the B:T163F mutation had no polar effect on the transcription of *fbcFBC*. In addition, since among the various mutations at position 163 only the F and P substitutions affected the assembly of the bc_1 complex (*9*), it was concluded that the defect observed in the latter mutants was post-translational.

Molecular Nature of the Ps^+ Revertants of the B:T163F Mutant. Ps^+ revertants of B:T163F were then sought to provide further insight into the molecular nature of the events leading to the absence of the bc_1 complex in this unusual mutant. The revertants were isolated and their molecular

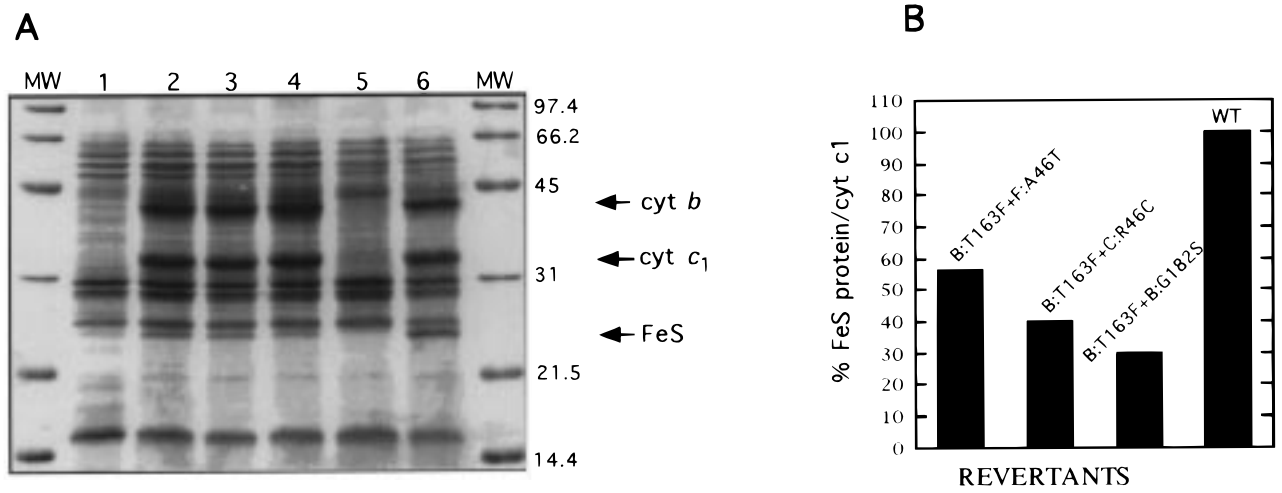

FIGURE 3: (A) Subunit composition of the bc_1 complex in the B:T163F mutant and in its revertants. Chromatophore membranes (35 μg) were treated with SDS−PAGE loading buffer at 37 °C for 15 min and analyzed by SDS−PAGE (15%): lane 1, MT-RBC1(bc_1^-); lane 2, B:T163F+F:A46T; lane 3, B:T163F+C:R46C; lane 4, B:T163F+B:G182S; lane 5, B:T163F; and lane 6, pMT0-404 (wild-type). Molecular mass markers (in kilodaltons) were from Bio-Rad. (B) Ratio of the Fe−S protein subunit to cyt c_1 in the B:T163F revertants. A gel similar to that shown in panel A was scanned; the pic area corresponding to appropriate bands was measured using the IP-GEL software program (Molecular Dynamics), and the values obtained were calibrated for their molecular masses and normalized to a cyt *b*/cyt c_1 ratio of 1. The percentage value for the Fe−S protein subunit per cyt c_1 thus determined is plotted in each case.

nature was analyzed as described in Materials and Methods. Two extragenic and one intragenic second-site suppressor mutations, A46T, R46C, and G182S located in the Fe−S protein, cyt c_1, and cyt *b* subunits, respectively, were found (Figure 2). The suppressor mutants B:T163F+B:G182S, B:T163F+C:R46C, and B:T163F+F:A46T and their derivatives carrying only the second-site mutations (B:G182S, F:A46T, and C:R46C constructed as described in Materials and Methods) were retained for further analysis.

Phenotypic Characterization of the B:T163F Revertants. The double mutants B:T163F+B:G182S, B:T163F+C:R46C, and B:T163F+F:A46T formed smaller colonies under Ps growth conditions and exhibited slightly longer doubling times (Ps growth rates in MPYE-enriched medium were 170, 210, and 150 min, respectively, vs 120 min for a wild-type strain). On the other hand, the single mutants carrying the second-site suppressor mutations B:G182S and F:A46T had growth rates almost identical to that of a wild-type strain while that of C:R46C was slightly slower (Table 1). Reduced *minus* oxidized optical difference spectra of the chromatophore membranes of all revertants were virtually identical to those of a wild-type strain (data not shown), and SDS−PAGE (Figure 3A) and Western blot analyses (data not shown) indicated that they contained wild-type amounts of cyt *b* and cyt c_1 subunits. However, the amount of the Fe−S protein found in chromatophore membranes of these mutants was variable and considerably lower than that in a wild-type strain (Figure 3B). For example, B:T163F+B:G182S contained as little as 30% Fe−S protein by protein staining or immunoblotting (see below). The single suppressor mutants B:G182S and C:R46C also exhibited lower amounts of the Fe−S protein (data not shown).

Steady-State and Single-Turnover Kinetics of the B:T163F Revertants. The double mutants exhibited significantly lower amounts of steady-state DBH-dependent cyt *c* reductase activities which were variable from 3 to 20% of that of a wild-type strain (Table 1). Furthermore, they also had slower single-turnover kinetics. In B:T163F+B:G182S and B:T163F+C:R46C, the electron transfer rates from Q_o to b_H in the presence of antimycin A were approximately 108 and 98 s^{-1} at E_hs of 100 and 106 mV and 38 and 35 s^{-1} at E_hs of 180 and 200 mV, respectively. Equally, the cyt c_1 re-reduction rates in these mutants were approximately 55 and 45 s^{-1}, respectively. These rates were about 4-fold slower than those observed with a wild-type strain (500 s^{-1} at an E_h of 116 mV and 118 s^{-1} at an E_h of 208 mV from Q_o to b_H in the presence of antimycin and 240 s^{-1} at an E_h of 106 mV for cyt c_1 re-reduction) (Table 1). In addition, in these strains, the amplitudes of the signal for cyt *b* reduction, or cyt *c* re-reduction, normalized to the amount of RC were also smaller (not shown), consistent with the substoichiometry of their Fe−S protein subunits. On the other hand, in the double mutant B:T163F+F:A46T and the single mutants F:A46T, C:R46C, and B:G182S, these rates were affected much less (Table 1).

Next, the EPR g_y signal of the [2Fe-2S] cluster of the Fe−S protein (Figure 4A) was used to semiquantitatively estimate its stoichiometry in mutant bc_1 complexes. This analysis revealed that B:T163F+B:G182S and B:T163F+C:R46C mutants had significantly smaller EPR g_y signals per the amount of total membrane proteins (Figure 4B) than a wild-type strain. Again, the B:T163F+F:A46T double and B:G182S and C:R46C single mutants had about 2-fold less, while F:A46T had almost wild-type levels of EPR g_y signals. The EPR spectra, in combination with the SDS−PAGE data described above, illustrated the fact that the second-site suppressor mutations located in cyt *b* and cyt c_1 restored less effectively the stoichiometry of the Fe−S protein subunit. Furthermore, the revertants B:T163F+B:G182S and B:T163F+C:R46C also exhibited weaker EPR g_x signals at $g = 1.80$ when the Q_{pool} was fully oxidized, indicating that their Q_o sites were also partially occupied, unlike the double mutant B:T163F+F:A46T and the single mutants B:G182S, C:R46C, and F:A46T (Figure 4A). Thus, among the three second-site suppressor mutations, the one located on the Fe−S protein was most efficient in overcoming the defect inflicted by the B:T163F mutation.

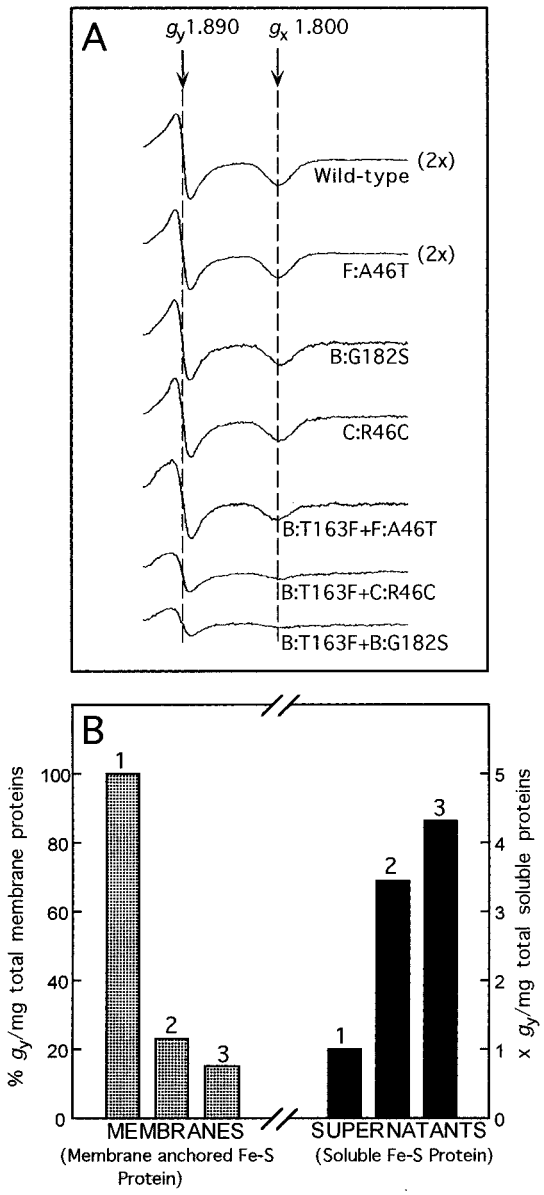

FIGURE 4: (A) EPR spectra of the B:T163F revertants and their single mutants. Chromatophore membranes were reduced using sodium ascorbate (20 mM), and the spectra, calibrated per total amount of membrane proteins, were obtained as described in Materials and Methods. (2x) refers to a 2-fold larger ordinate scale used for recording the wild-type and F:A46A spectra. The EPR conditions used were as follows: modulation amplitude, 12.5 G; microwave frequency, 9.49 GHz; microwave power, 2 mW; and modulation frequency, 100 kHz. (B) Relative amounts of the Fe−S protein subunit in the B:T163F revertants either remaining anchored to the chromatophore membranes (shown as a percentage of the wild-type EPR g_y signal per milligram of total membrane proteins) or becoming soluble in the supernatants of chromatophore membranes (shown as *x*-fold times the wild-type EPR g_y signal per milligram of total soluble proteins). The numbers 1−3 correspond to the *R. capsulatus* wild-type (pMTO-404/MT-RBC1), B:T163F+C:R46C, and B:T163F+B:G182S strains, respectively.

The Substoichiometry of the Fe−S Protein Subunit in B:T163F Revertants Is Not Induced by Increased Susceptibility of the [2Fe-2S] Cluster to Oxidative Damage. The low bc_1 complex activity found in the double mutants was unstable (although to a lesser extent in B:T163F+F:A46T) and often vanished within 2−3 days upon storage at 4 °C, unlike the wild-type activity which was stable over a period of 10 days under the same conditions. This observation led us to examine whether in these mutants the [2Fe-2S] cluster was more susceptible to oxidative damage upon exposure to air, as recently seen with several Fe−S protein mutants (*28*). For this purpose, the weakly suppressed double mutant B:T163F+B:G182S was chosen for further analysis (Figure 5). When the chromatophore membranes were prepared in the presence of 0.16 mg/mL sodium dithionite from anaerobically (Ps) grown cells of this mutant, the bc_1 complex activity was at most 2-fold higher than that observed in the membranes derived from respiratory-grown cells of the same mutant. In addition, when the ratio of the EPR g_y signal to the amount of the Fe−S protein per total protein (estimated by SDS−PAGE) was determined, no more than a 15−20% difference was found between the values obtained using Ps- or Res-grown cells of a given mutant (Figure 5A,B). Thus, although a slight increase in the susceptibility of the [2Fe-2S] cluster to oxidative damage could be detected, this was not sufficient to account for the low and variable amount of the Fe−S protein found in the B:T163F revertants.

A Soluble Form of the Rieske Fe−S Protein. We reasoned that the substoichiometry of the Fe−S protein subunit in B:T163F+B:G182S and B:T163F+C:R46C (Figure 3) may be due to its proteolytic degradation. If this were the case, then its degradation products could be detected in the supernatants of chromatophore membranes. Indeed, upon analysis of concentrated membrane-free supernatants by SDS−PAGE and immunoblotting, a 20 kDa polypeptide was readily recognized by monoclonal antibodies specific for the *R. capsulatus* Fe−S protein (*29*) (Figure 6). This band was also present, but to a much lesser extent, in the chromatophore membranes of both the wild-type strain pMT0-404/MT-RBC1 overproducing the bc_1 complex and the single mutants B:G182S, C:R46C, and F:A46T (data not shown). Conversely, the double mutants B:T163F+B:G182S and B:T163F+C:R46C contained approximately 3−5-fold higher amounts of this protein in the supernatants of the chromatophore membrane supernatants, while they exhibited similarly decreased amounts of the Fe−S protein in their chromatophore membranes (Figure 4B). The supernatants used in these experiments were devoid of membrane fragments, as confirmed by the absence of cyt c_1 using specific antibodies (data not shown).

The EPR g_y signal corresponding to the [2Fe-2S] cluster of the Fe−S protein could be readily detected in the supernatants of the chromatophore membranes prepared from the revertants B:T163F+B:G182S (Figure 7, inset) and B:T163F+C:R46C (data not shown). This signal was very similar to that observed in chromatophore membranes (Figure 4A), indicating that the Fe−S protein detected in the supernatants contained a wild-type-like [2Fe-2S] cluster. Furthermore, the soluble form of the Fe−S protein could not respond to stigmatellin and had no pronounced EPR g_x signal at $g = 1.80$ as shown earlier for the soluble bovine subunit (*30*). Potentiometric titration of the corresponding EPR g_y signal indicated that the E_{m7} values of the membrane-bound Fe−S protein subunit present in intact bc_1 complexes and that found in a soluble state in chromatophore supernatants were identical (about 285 mV for B:T163F+B:G182S) (Figure 7).

Next, the soluble form of the Fe−S protein was immunoprecipitated from the membrane-free supernatants of chromatophore membranes of B:T163F+B:G182S using specific

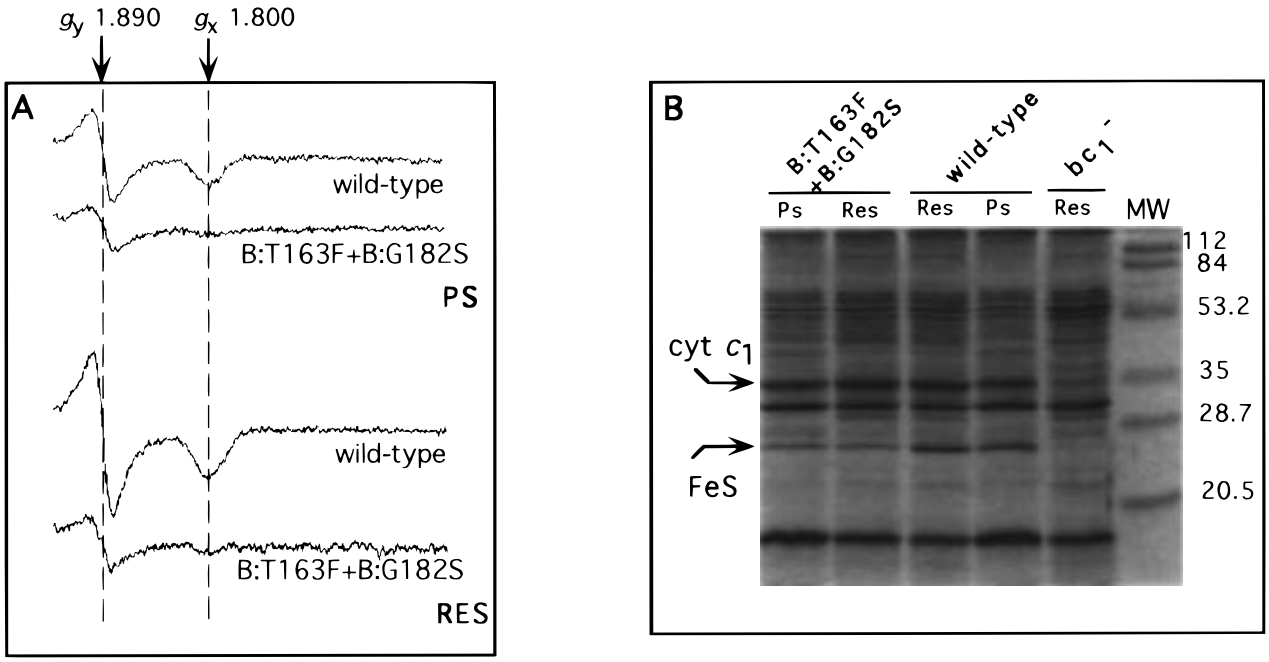

FIGURE 5: Amount of the [2Fe-2S] cluster per cyt c_1 in B:T163F+B:G182S mutant cells grown by photosynthesis or respiration. (A) EPR spectra of sodium ascorbate-reduced chromatophore membranes derived from wild-type and B:T163F+B:G182S cells grown by photosynthesis (Ps) or respiration (Res). The same amounts of membrane proteins (15.6 mg/mL) were used in each case, and the EPR conditions were as described in the legend of Figure 4. (B) SDS−PAGE (17%) of chromatophore membranes obtained from wild-type and B:T163F+B:G182S cells as described in panel A. Samples were prepared in SDS−PAGE loading buffer and incubated for 15 min at 65 °C. Under these conditions, cyt *b* aggregates and does not enter the gel while the Fe−S protein subunit runs as a single band of approximately 24 kDa.

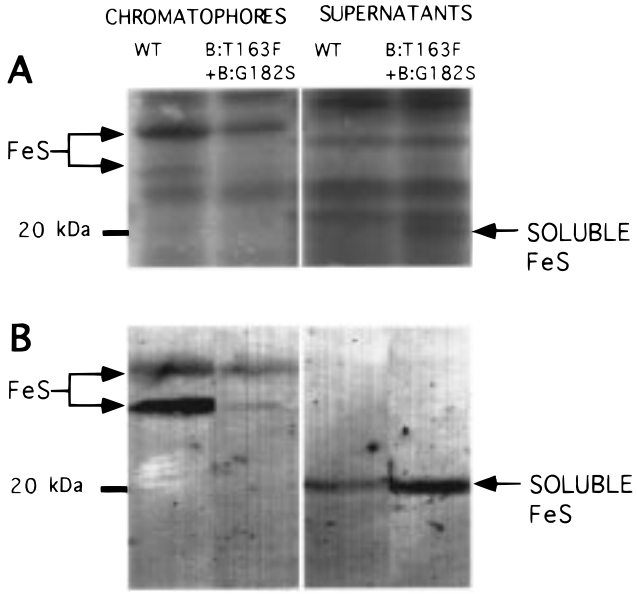

FIGURE 6: Soluble and membrane-bound forms of the Fe−S protein subunit of the bc_1 complex. (A) SDS−PAGE of chromatophore membranes and chromatophore membrane supernatants of the B:T163F+B:G182S mutant and its wild-type (WT) parent prepared as described in Materials and Methods. The gel conditions were as described in the legend of Figure 3. Note that the soluble form of the Fe−S protein subunit present in membrane supernatants of B:T163F+B:G182S can be detected (though barely) even by Coomassie staining. (B) Western blot analysis of the samples shown in panel A using monoclonal antibodies D39 specific for the *R. capsulatus* Fe−S protein clearly reveals the presence of this soluble form of the Fe−S protein.

monoclonal antibodies and purified by SDS−PAGE, and its amino-terminal amino acid sequence was determined as described earlier (*29*). The data obtained revealed that the soluble form of the Fe−S protein started with a valine followed by a KAMASIFVDVSAV sequence identical to positions 44−57 of its membrane-bound form. We therefore concluded that this subunit was cleaved between its amino acid residues aspartate (D) 43 and valine (V) 44, hence releasing it from the membrane, and rendering it sub-stoichiometric in the bc_1 complex. It was noticed that no further degradation of the cleaved portion of the Fe−S protein was observed, indicating that it must be folded properly to resist further proteolysis.

DISCUSSION

Detailed biochemical and genetic analyses of an unusual mutation located at position 163 of cyt *b* allowed us to reveal specific interactions between the subunits of the bc_1 complex around non-transmembrane helix *cd*1 of cyt *b*. Earlier, intragenic second-site suppressor mutations located in the subunits of the bc_1 complex have been reported, and the information obtained was useful in delimiting the interactions within them (*8*, *31*, *32*). In this work, extragenic second-site suppressor mutations between the different catalytic subunits of the bc_1 complex were studied in detail.

Various cyt *b* mutations affecting the assembly, or the steady-state stability, of the bc_1 complexes have been described previously. In bacteria, the amino acid residues located near the packing domains of the heme groups have severe effects, like the G48D substitution located near heme b_H (*33*) or the R114Q substitution located at the beginning of the *bc* loop between the helices B and C of cyt *b* (*34*). In yeast mitochondria, two cyt *b* mutations, L282F (305 in *R. capsulatus*) located near the highly conserved PEWY sequence and G304E predicted to be buried in the membrane, lacked the bc_1 complex (*35*). In addition, slight perturbations of the assembly of the bc_1 complex have been observed with mutations at positions 137 and 256 (152 and 279 in *R.*

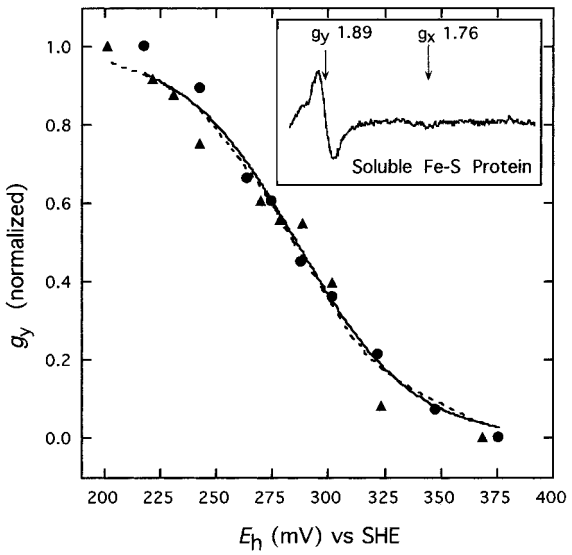

FIGURE 7: EPR redox titrations of chromatophore membranes and chromatophore membrane supernatants of the B:T163F+BG182S mutant grown by respiration. Redox titration for the [2Fe-2S] cluster of the Fe−S protein was performed by adding aliquots of sodium ascorbate in the presence of 10 μM TMPD and 50 μM 1,2-NQ-4S. The amplitude of the g_y signal was recorded at various E_h values, normalized, and fitted to an $n = 1$ Nernst equation: (●, — fit) the membrane-bound form of the Fe−S protein (chromatophore membranes, 21.7 mg of protein/mL) and (▲, ⋯ fit) the soluble form of the Fe−S protein (chromatophore membrane supernatants, 12.2 mg of protein/mL). EPR conditions were as described in the legend of Figure 4 except that the microwave power was 5 mW. The inset shows a sodium ascorbate-reduced EPR spectrum of chromatophore supernatants (10.8 mg/mL) of the B:T163F+B:G182S mutant, and the EPR conditions were as follows: modulation amplitude, 20 G; microwave frequency, 9.49 GHz; microwave power, 10 mW; and modulation frequency, 100 kHz.

capsulatus) located in the *cd*1 and *ef* loops of yeast cyt *b*, respectively (*20*, *36*). However, the B:T163F mutation described here appears to be unique. Its effect is clearly post-translational and allele-specific, since among the several substitutions available at this position only F and P are deleterious (*9*). Indeed, use of the *lacZ* fusions indicated that the B:T163F mutation has no significant effect on the transcription of the *fbcFBC* operon. Furthermore, the upstream and downstream locations of the second-site suppressor mutations in *fbcFBC* are consistent with the lack of any effect of B:T163F on the translation of the bc_1 complex subunits.

Our earlier work on the steady-state stability of the bc_1 complex (*23*) suggested that the B:T163F mutation must somehow affect not only the interactions between the Fe−S protein subunit and cyt *b* but also those between cyt *b* and cyt c_1 subunits to abolish the assembly of all subunits. Examination of the three-dimensional structure of the chicken heart bc_1 complex resolved by Berry and co-workers (*45*) indicated that the mitochondrial counterparts of *R. capsulatus* position B:T163 (i.e., T148 in the mitochondrial structure) and its suppressors, B:G182 (i.e., G167) and F:A46 (i.e., A70), described here are close to each other (Figure 8A). It is noteworthy that both of the two independent suppressor mutations reintroduce a hydroxyl group, suggesting that such a group may be necessary for the proper assembly of the bc_1 complex. However, these residues are not within hydrogen bonding distances of each other (Figure 8B), and various other substitutions at position 163, like V, L, I, and A, also yield inhibitor-resistant mutants (*9*). Thus, perhaps it is the presence of a bulky aromatic side chain (such as that of F) that abolishes the steady-state presence of the bc_1 complex in chromatophore membranes. On the other hand, the third suppressor position in the cyt c_1 subunit of *R. capsulatus*, C:R46 (i.e., R28 in the mitochondrial structure), is located remarkably far from B:T163 (i.e., B:T148) and also from the other suppressor positions in the bc_1 complex structure from the chicken heart mitochondria (Figure 8A) (*18*). How this mutation, which behaves as a global suppressor, compensates for the assembly defect of the bc_1 complex at such a distance is at present unclear. A possibility is that perhaps the overall folding of *R. capsulatus* cyt c_1 is distinct from that of its mitochondrial counterpart, which is unlikely in light of their pronounced homologies. Nonetheless, it would be of interest to define the exact location of C:R46C of cyt c_1 in the structure of the bc_1 complex from *R. capsulatus* when it becomes available.

Of the suppressor positions, G182 of cyt *b* is highly conserved in all species while R46 of cyt c_1 is only present in the bc_1 complexes and substituted with hydrophobic residues in the b_6f complexes (*4*). Position A46 of the Fe−S protein is also conserved in all Fe−S proteins except in those of some cyanobacteria. However, none of these residues is essential for either the structure or function of the bc_1 complex since their introduction into an otherwise wild-type background has no deleterious effect. Finally, we note that the Ps^+ revertants of B:T163F must restore both the assembly of the bc_1 complex and the function of its Q_o site, and further dissection of these two intertwined effects needs appropriate triple mutants. In this respect, noteworthy is the fact that the only triple mutant so far available, B:T163F+F:L136G+F:A46T, compensates preferentially for the assembly defect of the bc_1 complex and not the functional impairment of its Q_o site (G. Brasseur and F. Daldal, unpublished data).

A soluble Fe−S protein subunit similar to that encountered in this work has been obtained earlier from purified *Neurospora crassa* or the beef heart mitochondrial bc_1 complex by using limited chymotrypsin (*37*, *38*) or trypsin (*39*) digestion in vitro. Recently, a soluble form of the Fe−S protein subunit has also been obtained from beef heart mitochondria (*30*) using thermolysin which cleaves it at position V68 (corresponding to V44 in *R. capsulatus*), and its three-dimensional structure has been solved by Iwata et al. (*40*). Finally, Zhang et al. (*41*) have also obtained a soluble Fe−S protein by proteolytic cleavage from the b_6f complex and solved its three-dimensional structure (*42*). On the other hand, obtaining a soluble form of the bacterial Fe−S protein subunit using molecular genetics has been difficult. While Van Doren et al. (*43*) have cloned and expressed the *R. sphaeroides fbcF* in *E. coli*, incorporation of undesired forms of iron−sulfur clusters into this apoprotein complicated this work. More recently, Holton et al. (*44*) have succeeded in expressing the *Nostoc* Fe−S protein subunit and reconstituting in vitro its correct [2Fe-2S] cluster. In this respect, the *R. capsulatus* strains described here, yielding considerable amounts of a soluble form of the bacterial Fe−S protein with its native [2Fe-2S] cluster, are of particular interest for future structural and functional studies of this protein.

Clearly, in the B:T163F revertants, the Fe−S protein subunit becomes more prone to cleavage from the bc_1 complex, although the nature of its cleaving agent, such as

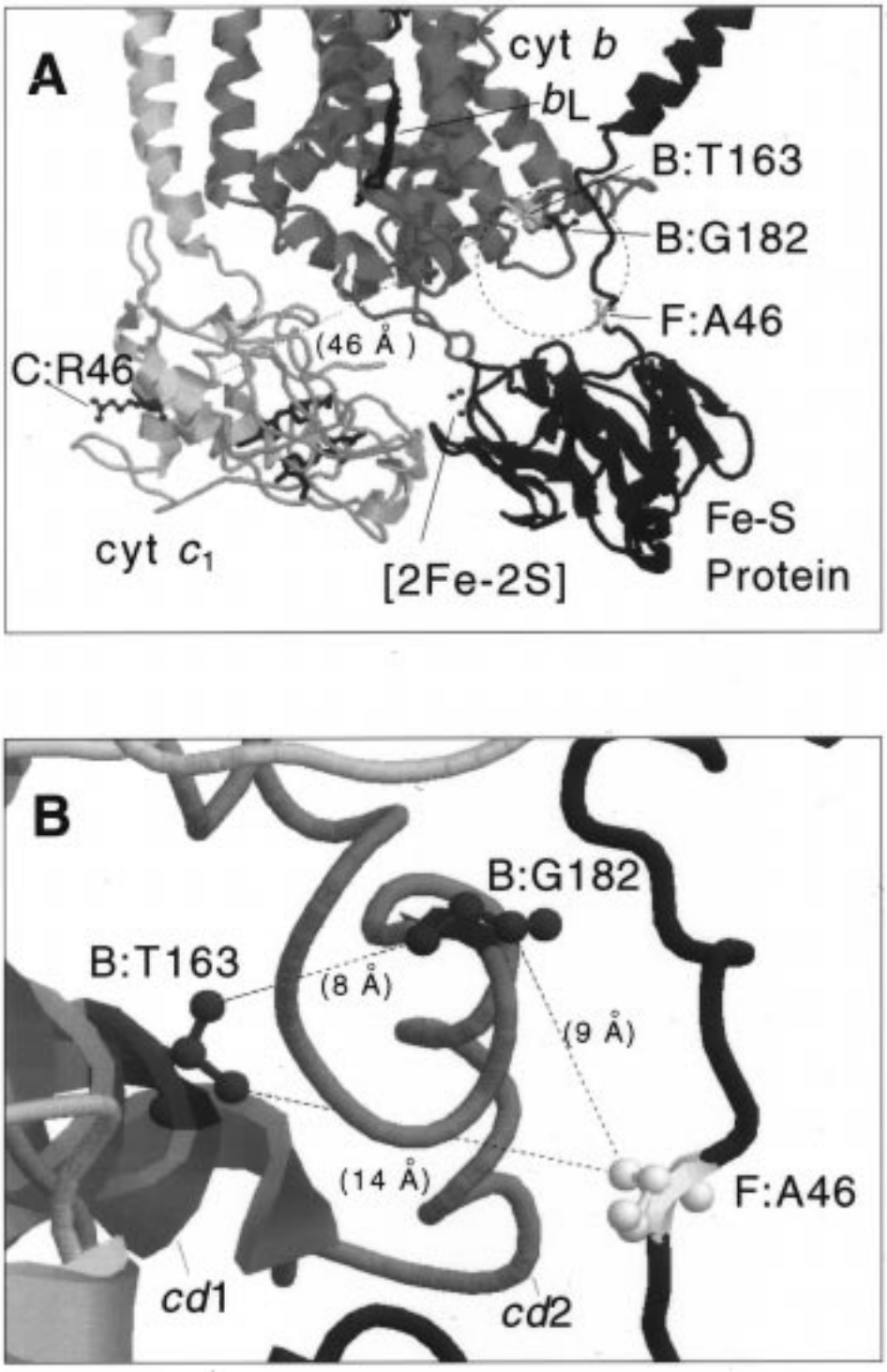

FIGURE 8: Model of the region surrounding position T163 of cyt *b* and the intra- and intergenic suppressor positions found in this work. The figures were generated and the closest distances between the amino acid residues measured using RasMol 2.6-ucb1.0 and the preliminary atomic coordinates of the bc_1 complex from chicken heart mitochondria. Panel A depicts the region encompassing residues B:T163 (i.e., T148 in the mitochondrial structure), B:G182 (i.e., G167), and F:A46 (i.e., A70) clustered together and C:R46 (i.e., R28 in the mitochondrial structure) which is far from the other positions. The [2Fe-2S] cluster, cyt b_L heme, and cyt c_L heme are also shown. Panel B depicts a closeup of the region encompassing residues B:T163 (i.e., T148 in the mitochondrial structure), B:G182 (i.e., G167), and F:A46 (i.e., A70), non-transmembrane helices *cd*1 and *cd*2 of cyt *b*, and the flexible "neck" region of the Fe−S protein subunit of the bc_1 complex.

for example a specific protease, remains unknown. To what extent this proteolysis takes place during cell growth in vivo or during preparation of the chromatophore membranes in vitro is also unclear. Its production may simply be amplified in B:T163F revertants since even in pMT0-404/MT-RBC1 overproducing the wild-type bc_1 complex small amounts of the cleaved product can be detected. In any event, it is important to underline the fact that the cleavage site (V44) is only two residues away from position 46 where the strongest of the suppressor mutations described here (F:A46T) is located. Moreover, intragenic suppressors of the L136G and -H mutations located next to the [2Fe-2S] cluster ligands of the Fe−S protein subunit (*28*) have also been found at both position 44 and 46 (*32*). Finally, recent

structural data suggest that this very same region might also mediate movement of the Fe−S protein subunit in response to stigmatellin (*17*−*19*, *45*). Therefore, the flexible amino-terminal portion of the Fe−S protein encompassing residues M_{62}SASADVLA_{70} (corresponding to M_{38}NASADVKA_{46} in *R. capsulatus*) is important not only for the assembly of the bc_1 complex but also for the structure and function of its Q_o site.

In conclusion, T163 of cyt *b* is the very first example of critical residues affecting cleavage of the Fe−S protein subunit at a region thought to be responsible for its mobility during Q_o site catalysis. Whether this cleavage will turn out to be the basis of a molecular mechanism regulating cellular energy transduction by proteolytic inactivation of the bc_1 complex remains to be seen.

ACKNOWLEDGMENT

We thank Drs. C. Slaugther and C. Moomaw of HHMI at the University of Texas Health Science Center at Dallas for amino acid sequence determination. We are grateful to Dr. B. R. Gibney for help with EPR measurement and to Dr. G. Brasseur for stimulating discussions.

REFERENCES

1. Gennis, R. B., Barquera, B., Hacker, B., Van Doren, S. R., Arnaud, S., Crofts, A. R., Davidson, E., Gray, K. A., and Daldal, F. (1993) *J. Bioenerg. Biomembr. 25*, 195−209.
2. Brandt, U., and Trumpower, B. (1994) *Crit. Rev. Biochem. 29*, 165−197.
3. Gray, K. A., and Daldal, F. (1995) in *Anoxygenic Photosynthetic Bacteria* (Blankenship, R. E., Madigan, M. T., and Bauer, C., Eds.) pp 725−745, Kluwer Academic Publishers, Dordrect, The Netherlands.
4. Degli-Esposti, M. D., De Vries, S., Crimi, M., Gelli, A., Patarnello, T., and Meyer, A. (1993) *Biochim. Biophys. Acta 1143*, 243−271.
5. Brasseur, G., Saribas, A. S., and Daldal, F. (1996) *Biochim. Biophys. Acta 1275*, 61−69.
6. Daldal, F., Tokito, M. K., Davidson, E., and Faham, M. (1989) *EMBO J. 8*, 3951−3961.
7. Robertson, D. E., Daldal, F., and Dutton, P. L. (1990) *Biochemistry 29*, 11249−11260.
8. Atta-Asafo-Adjei, E., and Daldal, F. (1991) *Proc. Natl. Acad. Sci. U.S.A. 88*, 492−496.
9. Tokito, M. K., and Daldal, F. (1993) *Mol. Microbiol. 9*, 965−978.
10. Ding, H., Moser, C. C., Robertson, D. E., Tokito, M. K., Daldal, F., and Dutton, P. L. (1995) *Biochemistry 34*, 15979−15996.
11. Ding, H., Daldal, F., and Dutton, P. L. (1995) *Biochemistry 34*, 15997−16003.
12. Saribas, A. S., Ding, H., Dutton, P. L., and Daldal, F. (1995) *Biochemistry 34*, 16004−16012.
13. Saribas, A. S., Ding, H., Dutton, P. L., and Daldal, F. (1997) *Biochim. Biophys. Acta 1319*, 99−108.
14. Yue, W.-H., Zou, Y.-P., Yu, L., and Yu, C.-A. (1991) *Biochemistry 30*, 2303−2306.
15. Kubota, T., Kawamoto, M., Fukuyama, K., Shizawa-Itoh, K., Yoshikawa, S., and Matsubara, H. (1991) *J. Mol. Biol. 221*, 379−382.
16. Berry, E. A., Huang, L.-S., Earnest, T. N., and Jap, B. K. (1992) *J. Mol. Biol. 224*, 1161−1166.
17. Xia, D., Yu, C. A., Kim, H., Xia, J.-Z., Kachurin, A. M., Zhang, L., Yu, L., and Deisenhofer, J. (1997) *Science 277*, 60−66.
18. Berry, E. A., Zhang, Z., Huang, L.-S., Chi, Y.-I., and Kim, S. H. (1997) *Biophys. J. 72*, A137.
19. Kim, H., Xia, D., Deisenhofer, J., Yu, C.-A., Kochurin, A., Zhang, L., and Yu, L. (1997) *FASEB J. 11*, A1084.
20. Giessler, A., Geier, B. M., di Rago, J.-P., Slonimski, P. P., and von Jagow, G. (1994) *Eur. J. Biochem. 222*, 147−154.
21. Mather, M. W., Yu, L., and Yu, C.-A. (1995) *J. Biol. Chem. 270*, 28668−28675.
22. Davidson, E., Ohnishi, T., Atta-Asafo-Adjei, E., and Daldal, F. (1992) *Biochemistry 31*, 3342−3358.
23. Davidson, E., Ohnishi, T., Tokito, M. K., and Daldal, F. (1992) *Biochemistry 31*, 3351−3358.
24. Gray, K. A., Davidson, E., and Daldal, F. (1992) *Biochemistry 31*, 11864−11873.
25. Ditta, G., Schmidhauser, T., Yakobson, E., Lu, P., Liang, X. W., Finlay, D. R., Guiney, D., and Helinski, D. (1985) *Plasmid 13*, 149−153.
26. Lowry, O. H., Rosebrough, N. J., Farr, A. L., and Randal, R. J. (1951) *J. Biol. Chem. 193*, 1571−1579.
27. Gray, K. A., Dutton, P. L., and Daldal, F. (1994) *Biochemistry 33*, 723−733.
28. Liebl, U., Sled, V., Brasseur, G., Ohnishi, T., and Daldal, F. (1997) *Biochemistry 36*, 11675−11684.
29. Robertson, D. E., Ding, H., Chelminski, P. R., Slaughter, C., Hsu, J., Moomaw, C., Tokito, M., Daldal, F., and Dutton, P. L. (1993) *Biochemistry 32*, 1310−1317.
30. Link, T. A., Saynovits, M., Assman, C., Iwata, S., Ohnishi, T., and von Jagow, G. (1996) *Eur. J. Biochem. 237*, 685−691.
31. di Rago, J. P., Hermann-Le Denmat, S., Paques, F., Risler, J. L., Netter, P., and Slonimski, P. P. (1995) *J. Mol. Biol. 248*, 804−811.
32. Brasseur, G., Sled, V., Liebl, U., Ohnishi, T., and Daldal, F. (1997) *Biochemistry 36*, 11685−11696.
33. Yun, C. H., Wang, Z., Crofts, A. R., and Gennis, R. B. (1992) *J. Biol. Chem. 267*, 5901−5909.
34. Hacker, R., Barquera, B., Gennis, R. B., and Crofts, A. R. (1994) *Biochemistry 33*, 13002−13031.
35. Lemesle-Meunier, D., Brivet-Chevillotte, P., di Rago, J. P., Bruel, C., Tron, T., and Forget, N. (1993) *J. Biol. Chem. 268*, 15628−15632.
36. Geier, B. M., Schaegger, H., Brandt, U., Colson, A. M., and von Jagow, G. (1992) *Eur. J. Biochem. 208*, 375−380.
37. Li, Y., DeVries, S., Leonard, K., and Weiss, H. (1981) *FEBS Lett. 135*, 277−280.
38. Romisch, J., Tropschung, M., Sebald, W., and Weiss, H. (1987) *Eur. J. Biochem. 164*, 111−115.
39. Gonzalez-Halpen, D., Vazquez-Acevedo, M., and Garcia-Ponce, B. (1991) *J. Biol. Chem. 256*, 3870−3876.
40. Iwata, S., Saynovits, M., Link, T., and Michel, H. (1996) *Structure 4*, 567−579.
41. Zhang, H., Carrell, C. J., Huang, D., Sled, V., Ohnishi, T., Smith, J. L., and Cramer, W. A. (1996) *J. Biol. Chem. 271*, 31360−31369.
42. Carrel, C. J., Zhang, H., Cramer, W. A., and Smith, J. L. (1997) *Structure 5*, 1613−1625.
43. Van Doren, S. R., Yun, C.-H., Crofts, A. R., and Gennis, R. B. (1993) *Biochemistry 32*, 628−636.
44. Holton, B., Wu, X., Tsapin, A. I., Kramer, D. M., Malkin, R., and Kallas, T. (1996) *Biochemistry 35*, 15485−15493.
45. Zhang, Z., Huang, L., Shulmeister, V. M., Chi, Y.-I., Kim, K. K., Hung, L.-W., Crofts, A. R., Berry, E. A., and Kim, S.-H. (1998) *Nature 392*, 677−684.

BI973146S